

Cutting a Pancake with an Exotic Knife

David O. H. Cutler
Mathematics Department
Tufts University
Medford, MA 02155
Email: david.cutler@tufts.edu

Neil J. A. Sloane¹
The OEIS Foundation Inc.
Highland Park, NJ 08904
Visiting Scholar, Math. Dept.
Rutgers University
Piscataway, NJ 08854
Email: njasloane@gmail.com

Abstract

In the first chapter of their classic book *Concrete Mathematics*, Graham, Knuth, and Patashnik consider the maximum number of pieces that can be obtained from a pancake by making n cuts with a knife blade that is straight, or bent into a V, or bent twice into a Z. We extend their work by considering knives, or “cookie-cutters”, of even more exotic shapes, including a k -armed V, a chain of k connected line segments, a long-legged version of one of the letters A, E, L, M, T, W, or X, a convex polygon, a circle, a figure 8, a pentagram, a hexagram, or a lollipop. In many cases a counting argument combined with Euler’s formula produces an explicit expression for the maximum number of pieces. “Strict” versions of the letters A and T are also considered, for which we have only conjectural formulas.

*Like a long-legged fly upon the stream
His mind moves upon silence.*

W. B. Yeats, *Long-Legged Fly* [13]

1 Introduction

A standard problem in combinatorial geometry specifies a two-dimensional shape S (a line, a circle, a triangle, etc.) and asks for the value of $a_S(n)$, the maximum number of regions that the plane can be divided into by drawing n copies of S . The copies of S can be individually rescaled, rotated, reflected, and sometimes (for example if S is an ellipse) stretched.

If S is an infinite straight line (or knife) K , we get the classical pancake-cutting problem [2, pp. 72–73], [3, Ch. 20], [4, §1.2], [12, p. 13, Problem 44], for which the answer is that the maximum number of pieces of an infinite pancake that can be obtained with n cuts is

$$a_K(n) = n(n+1)/2 + 1. \tag{1}$$

¹To whom correspondence should be addressed.

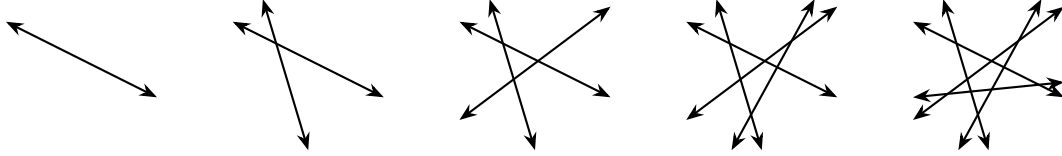


Figure 1: Cutting an infinite pancake with 1, 2, 3, 4, or 5 cuts using an infinite straight knife produces a maximum of 2, 4, 7, 11, or 16 pieces. Arrowheads indicate infinite lines.

We give a proof and an explicit construction in §2. The numbers $a_{\kappa}(n), n \geq 0$, form entry [A000124](#) in the *On-Line Encyclopedia of Integer Sequences* (or *OEIS*) [10]. (Six-digit numbers prefixed by A will always refer to entries in the OEIS.) Figure 1 shows solutions for $1 \leq n \leq 5$ cuts.

When we began this investigation, the OEIS already contained several other sequences of this type. The following list includes both pre-existing and new sequences. An asterisk * indicates a sequence which was not hitherto associated with a dissection problem. We believe that our solutions (or, in four cases, attempted solutions) to the problems indicated by the asterisks are new.

The sequences, associated shapes S , and section numbers if they are mentioned in this article are: [A000124](#) (S is a line, §2), [A000125](#) (plane in three dimensions), [A046127](#) (sphere in three dimensions), [A051890](#) (ellipse), [A058331](#) (hyperbola), [A069894](#) (square or convex quadrilateral, §8.1), [A077588](#) (triangle, §1), [A077591](#) (concave quadrilateral), [A080856*](#) (4-chain, §5), [A117625](#) (Z or zig-zag, §7), [A125201*](#) (W or M, §7), [A130883](#) (V, §4), [A140064*](#) (A, E, 3-armed V, 3-chain, Wu (W), or Shah (Ш), §§4, 6), [A143689*](#) (constrained L, §8.1), [A330451*](#) (constrained A, §9.2), [A383464*](#) (4-armed V, §4), [A383465*](#) (5-chain, §5), [A383466*](#) (pentagram, §10.5), [A383477*](#) (hexagram, §10.5), [A386480](#) (circle, §10.3), [A386485*](#) (pentagon, §10.1), [A386486*](#) (8, §10.4), [A389608*](#) (lollipop (P), §11), and [A389614*](#) (constrained T, §9.1). In a few cases, where we do not know the exact number of regions, the sequence mentioned is the best upper bound presently known. The second and third entries in the above list, [A000125](#) and [A046127](#), are the only three-dimensional problems.

We will give references to the OEIS throughout this article, for several reasons. One is that, apart from [4], most of the previous work on these problems first appeared in the OEIS rather than in a journal. We would appreciate hearing of any references we have overlooked, especially for the more exotic shapes. Another reason is that the OEIS entries include the initial terms of the sequence, additional formulas and illustrations, references, etc.

As we shall see, the OEIS also led us to make two unexpected discoveries. First, the numbers of regions formed with n copies of any of the long-legged letters A, a three-armed V (or Wu or Shah), or a 3-chain are all equal (§§4, 5, 6). Second, the numbers of regions formed by n octagons or by n concave quadrilaterals are equal (§10.2). For the first we give a geometric explanation, whereas the second *may* be simply a coincidence caused by the fact that the same formula arose in two different but closely related contexts.

The three cases when S is a line, or a bent line in the form of a V with two very long

limbs



or a “zig-zag”, a doubly bent line in the form of a Z with two long parallel limbs joined by a diagonal line segment



are discussed in the first chapter of Graham, Knuth, and Patashnik’s *Concrete Mathematics* [4]. In order to generalize their examples, we observe that they may be regarded as “long-legged” versions of the upper-case letters I, V, and Z. (The term was suggested by W. B. Yeats’s poem in praise of silence, *Long-Legged Fly* [13, pp. 327–328].)

This led us to consider long-legged versions of other letters. Informally, a long-legged version of a letter is obtained by replacing any protruding arms or legs by (semi-infinite) rays, indicated by arrow-heads, and allowing arbitrary angles between these rays. For example there is no restriction on the angle between the two arms of a long-legged V. We will, of course, be careful to give a precise definition for each shape. There are interesting long-legged versions of A, E, L, M, T, W, and X, sometimes more than one. Curved letters (B, C, D, G, P, Q, R, S, . . .) do not seem appropriate for this treatment, since as we shall show below, once curved lines are permitted (without any bound on their curvature), it is easy to create arbitrarily many regions. The curved shapes O (§10.3), 8 (§10.4) and the lollipop (§11) are exceptions. A cookie-cutter in the shape of a long-legged A initially looked especially challenging, although as we shall see in §6, it has a surprisingly simple solution. The constrained long-legged \bar{A} , however (§9.2), appears to be genuinely hard.

Long-legged versions of some letters (L, X, Y, among others) are potentially interesting, but because our rules allow arbitrary angles between the extended legs, they would be indistinguishable from other letters. An L would be the same as a V, for example. We therefore define a class of “constrained” long-legged letters, indicated by a bar over the letter, which impose additional conditions. Examples will be found in Sections 8 and 9.

These constrained letters appear to be more difficult to analyze, and we will therefore divide the shapes we consider into two families. Members of what we will call the *affine* family of shapes have the property that if S is a shape of that type, so is any image of S under the full two-dimensional affine group \mathcal{G}_{aff} generated by linear transformations (which need not be isometries), followed by a translation. On the other hand, the *similarity* family of shapes have the property that if S is a shape of that type, so is any image of S under the group \mathcal{G}_{sim} of two-dimensional similarities, generated by isometries (rotations, reflections, translations), followed by a dilation. The affine shapes we consider are the line, the hatpin, the k -armed V, the k -chain, the long-legged letters A, M, W, Z (§§2-7), and the convex polygon (§10.1). All the other shapes belong to the similarity family.

We analyze these shapes by studying the planar graph formed by the union of the copies of the shape. We describe this graph, denoted by $G_S(n)$ if there are n copies of S , in §2, using the case when S is a line as an example.

Subsequent sections will then discuss other shapes, beginning with the half-line or ray (§3). To emphasize the difference between a line and a ray, we refer to a ray as a *hatpin* (see Fig. 6).

The next-simplest shape after the hatpin is the V , and in §4 we will analyze a long-legged k -armed V for $k \geq 2$. The three-armed V is particularly interesting. It is called a Wu (\mathbb{V}), and is included in the Unified Canadian Aboriginal Syllabics section of Unicode, where it has the symbol U+2A5B. The Wu has also been called a Boolean OR with a middle stem. The number of regions obtained from a long-legged E or Shah (\mathbb{U}) turns out to be the same as for a Wu, so we simply define long-legged E 's and Shah's to be long-legged Wu's.

Subsequent sections are devoted to a k -chain (§5), and long-legged versions of A (§6), Z , W , and M (§7), and the constrained long-legged letters \bar{L} and \bar{X} (§8), and \bar{T} and \bar{A} (§9). We study several finite shapes in §10, namely a convex k -sided polygon (§10.1, §10.2), a circle (§10.3), a figure 8 (§10.4), and a regular pentagram and hexagram (§10.5). Our final shape is a lollipop (\mathbb{P}) (§11).

Our methods can be applied to many shapes besides these, and could be used to provide proofs for many formulas stated without proof in the OEIS entries mentioned in our initial list.

The final section lists some open problems. One in particular is worth emphasizing: is there any connection between the present work and the classical subject of “Geometrical Configurations” [6, 7, 9]? Many of our graphs are in fact geometrical configurations, so it is natural to wonder if any results from the classical literature can be applied to our problem.

For the “affine” shapes we consider (and for most of those on the list at the start of this Introduction), $a_S(n)$ grows quadratically with n . For triangles (A077588), for example, $a_S(n) = 3n^2 - 3n + 2$ for $n \geq 1$. It is possible, however, for $a_S(n)$ to grow much more rapidly than this. For example, Grünbaum's n -set Venn diagram construction [5, 11] (see Fig. 2 for $n = 6$), shows that if S is a simple Jordan curve, a snake or sausage shape, for example, we can achieve $a_{JC}(n) \geq 2^n$. In fact, $a_{JC}(2)$ is already unbounded, since it can be made as large as we please by intertwining two snakes (as in drawings of a caduceus). Of course the very definition of a Jordan curve implies $a_{JC}(1) = 2$. But even $a_S(1)$ itself can be arbitrarily large if S is a twisted sausage (Fig. 3). To avoid such complications, we will mostly only consider polygonal shapes.

Notation. In order to distinguish between the letters themselves and the symbols denoting their properties, we will use a *sans serif* font (A, L, V , etc.) for the letters and other shapes. We use K for the infinite knife-cuts in the basic pancake-cutting problem, H for the hatpin, kV for the k -armed V , kC for the k -chain, and kP for the k -sided polygon. An overbar (\bar{L} , \bar{X} , etc.) indicates a constrained shape.

For a shape S , $G_S(n)$ is a graph formed by drawing n copies of S , and $a_S(n)$ is the maximum number of regions in the plane that can be obtained in this way. We will say that $G_S(n)$ is *optimal* if it has $a_S(n)$ regions. Red and black dots indicate base and crossing nodes, respectively.

The parameters of $G_S(n)$ will be denoted by $V_B, V_C, V = V_B + V_C$ (numbers of base nodes, crossing nodes, total vertices), $E_\infty, E_f, E = E_\infty + E_f$ (infinite edges, finite edges, total edges), and $R_\infty, R_f, R = R_\infty + R_f$ (infinite regions, finite regions, total regions). These definitions will be repeated when they appear below.

Also, $\sigma(S)$ is the maximum number of self-crossings in a single S , $\kappa(S)$ is the maximum number of intersections between two copies of S , and *cpa* is the average number of *crossing*

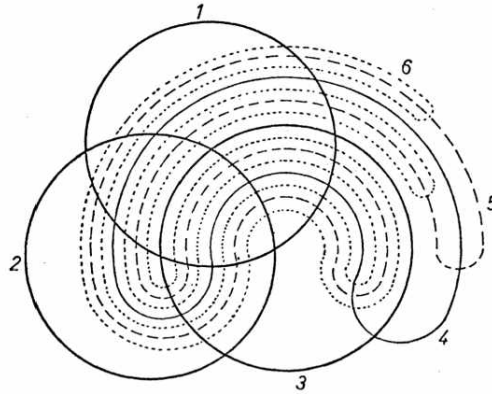


Figure 2: A 6-set Venn diagram (with 64 regions) constructed from six copies of a sausage shape S , from Grünbaum [5]. (A circle is a very simple sausage.) The construction easily generalizes to show that at least 2^n regions can be achieved using n copies of a simple Jordan curve.



Figure 3: A single twisted sausage shape can produce arbitrarily many regions.

nodes per arm.

2 The planar graph and the maximum number of regions

We start by thinking of our shape S itself as a planar graph with certain vertices and edges. We call its vertices *base nodes* and its edges *arms*. A long-legged V, for example, has a single base node and two arms. A k -chain (§5) has $k - 1$ base nodes and k arms. We denote the set of base nodes by \mathcal{B} , and the degree of $v \in \mathcal{B}$ by d_v , or by $d_{\mathcal{B}}$ if the degree is the same for all $v \in \mathcal{B}$.

The planar graph $G_S(n)$ for a drawing formed from n copies of S is then the union of the graphs for the individual copies, together with a new vertex for any point where a pair of arms cross, and new edges that replace the portions of the arms between the new vertices. We will refer to these new vertices as *crossing nodes*. In some drawings the base nodes are indicated by small red circles, and the crossing nodes by small black circles. (We have not done this in every drawing, to avoid clutter.)

The arms of a copy of S may themselves cross, and these *self-crossings* are also considered to be crossing nodes.

Since our goal is always to maximize the number of regions, we will assume that no crossings ever involve more than two arms, and no arm from one copy of S intersects a base node from a different S (for otherwise a small perturbation would increase the number of

regions).

Let $V_{\mathcal{B}}$ denote the total number of base nodes over all n copies of S , $V_{\mathcal{C}}$ the total number of crossing nodes, and $V = V_{\mathcal{B}} + V_{\mathcal{C}}$ the total number of vertices of $G_S(n)$. Let E_{∞} and E_f respectively denote the number of infinite and finite edges, and $E = E_{\infty} + E_f$ the total number of edges, and similarly let R_{∞} , R_f , and $R = R_{\infty} + R_f$ denote the numbers of infinite, finite, and total regions.

If S is bounded and $E_{\infty} = 0$, Euler's formula [1, p. 22], [8] for $G_S(n)$ tells us that

$$R - E + V = 2 . \quad (2)$$

This version of Euler's formula will be relevant in §10. But most of the shapes we analyze are infinite, with $E_{\infty} = R_{\infty} > 0$, in which case Euler's formula for the Euclidean (or affine) plane tells us that $G_S(n)$ satisfies

$$R - E + V = 1 . \quad (3)$$

We were surprised not to find (3) in Lakatos [8], a book devoted to proofs of different versions of Euler's formula, nor in the standard books on finite graph theory. But (3) is simple to prove. Draw a rectangle around $G_S(n)$, large enough so that only the E_{∞} edges cross it. The rectangle therefore has $4 + E_{\infty}$ edges and $4 + E_{\infty}$ vertices. The graph formed by the union of $G_S(n)$ and the rectangle has $E + 4 + E_{\infty}$ edges, $V + 4 + E_{\infty}$ vertices, and by (2) has $(E + 4 + E_{\infty}) - (V + 4 + E_{\infty}) + 1 = V - E + 1$ regions inside the rectangle.

Let us assume then that our shape S is a connected graph formed from straight line segments, some of which may be infinite. What greatly simplifies the analysis of these graphs is that there is a second equation linking E and V , which we obtain by counting edge-vertex incidences in two ways. On the left side of this equation we sum the degrees d_v of all the base nodes $v \in \mathcal{B}$ and add four times the number of crossing nodes. This will count each edge twice, except for the E_{∞} infinite edges, which will only be counted once, and so we add an extra term E_{∞} to the left side. On the right side we simply count each edge twice. The edge-vertex count then tells us that

$$\sum_{v \in \mathcal{B}} d_v + 4V_{\mathcal{C}} + E_{\infty} = 2(E_{\infty} + E_f) , \quad (4)$$

that is,

$$E_f = 2V_{\mathcal{C}} + \frac{1}{2} \sum_{v \in \mathcal{B}} d_v - \frac{1}{2} E_{\infty} . \quad (5)$$

By combining this with Euler's formula (3), we obtain our basic equation, which is

$$R = V_{\mathcal{C}} + \frac{1}{2} \sum_{v \in \mathcal{B}} d_v - V_{\mathcal{B}} + \frac{1}{2} E_{\infty} + 1 . \quad (6)$$

On the right side, only $V_{\mathcal{C}}$ depends on how the shapes are placed in the plane, the other quantities being determined by S and n , and so we deduce that, for the shapes we are considering,

$$\begin{aligned} &\text{to maximize the number of regions, it is necessary} \\ &\text{and sufficient to maximize the number of crossings.} \end{aligned} \quad (7)$$

We illustrate this by studying the classic pancake-cutting problem mentioned in the Introduction, for which the shape K (for “knife”) is an infinite straight line, such as the line $y = 0$, or any of its images under the affine group \mathcal{G}_{aff} . (To minimize the introduction of new symbols, we will abuse notation slightly and use the same symbol for both a single instance of the shape, and for the family of all such shapes.) K has no base vertices and one arm. We form the pancake graph $G_K(n)$ by drawing $n \geq 2$ such lines. We may assume that each line crosses at least one other line, so $V_B = 0$ and $E_\infty = 2n$. Equation (6) then says that

$$R = V_C + n + 1 . \quad (8)$$

We maximize V_C by making every pair of lines intersect, giving $V_C = \binom{n}{2}$, and so the maximum number of regions is $R = a_K(n) = \binom{n}{2} + n + 1$, establishing (1).

The underlying reason that (7) holds is that, because our shapes are built out of straight lines, locally the graphs have a tendency to look like a square mesh, with $E \approx 2V$ (cf. (5), (13)). This also explains why the associated sequences $a_S(n)$ have only piecewise quadratic growth.

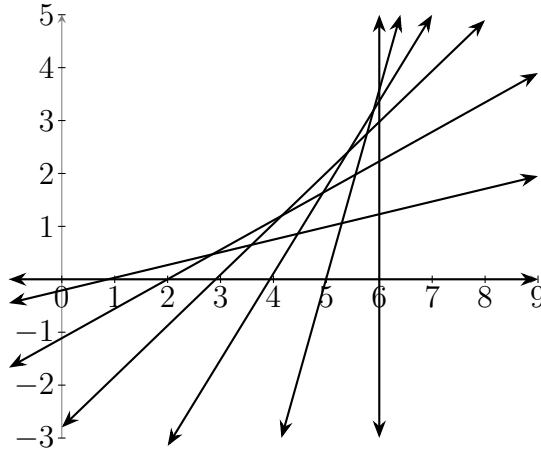


Figure 4: An optimal pancake graph $G_K(7)$ defined by (9) with $n = 6$ and $\theta = 15^\circ$. The $t = 0$ line is the x -axis, and the $t = 6$ line is $x = 6$.

Since the optimal pancake graph $G_K(n)$ is the basis for other constructions, we summarize its properties: $V = V_C = \binom{n}{2}$, $E_\infty = R_\infty = 2n$, $E_f = n(n - 2)$, $E = n^2$, $R_f = \binom{n-1}{2}$, and $R = a_K(n) = (n^2 + n + 2)/2$ (A000124). Our very first figure, Figure 1, shows some *ad hoc* drawings of these graphs. The following is an explicit construction of an optimal pancake graph with $N + 1 \geq 2$ lines. Let $\theta = \pi/(2N)$, and take the lines to have equations

$$(x - t) \sin t\theta = y \cos t\theta \quad \text{for } t = 0, 1, \dots, N . \quad (9)$$

Figure 4 illustrates the construction of a $G_K(7)$, taking $N = 6$.

For use in §10 we give the analog of our basic equation (6) that applies if the shape S is finite. Since $E_\infty = 0$, the equation is now

$$R = V_C + \frac{1}{2} \sum_{v \in \mathcal{B}} d_v - V_B + 2 . \quad (10)$$

We end this section by defining three parameters associated with S that are helpful when searching for optimal graphs. First, if the definition of S permits, it may be possible to move the arms of S so as to increase the number of self-crossings (this applies to the k -chain, for example). We let $\sigma(S)$ denote the maximum number of self-crossings in a single S .

Second, $\kappa(S)$ will denote the maximum number of intersections between two copies of S . With n copies of S , an upper bound on the total number of crossings is therefore

$$V_C \leq n\sigma(S) + \binom{n}{2}\kappa(S). \quad (11)$$

If equality holds in (11), the graph is optimal.

In most of the examples studied in this paper, we are able to achieve equality in (11). The chief difficulty, once we have determined $\kappa(S)$, lies in placing the n copies of S so that every pair intersect in $\kappa(S)$ points. We run into difficulties if, once one copy of S has been positioned, there are only a small range of possibilities for the second (and therefore *all*) subsequent copies. This is the case for the constrained letters \bar{T} (§9.1) and \bar{A} (§9.2), and for the figure 8 (§10.4) and the lollipop (§11).

This difficulty seems never to arise with any of our affine family of shapes, where there always seems to be a plentiful supply of candidates for the next copy of the shape. This leads us to make the following bold

Conjecture. If S is a shape belonging to the affine family, then equality can always be achieved in (11).

Third, by assumption, each crossing node is at the intersection of exactly two arms, and so the average number of crossings per arm (abbreviated *cpa*) is

$$cpa = \frac{2V_C}{\alpha(n)} \leq \frac{n\sigma(S) + \binom{n}{2}\kappa(S)}{\alpha(n)}, \quad (12)$$

where $\alpha(n)$ is the total number of arms. The *cpa* is not always an integer, even for optimal graphs (the k -chains for $k \geq 3$, for example). But if the right side of (12) is an integer, the *cpa* can be useful when searching for optimal graphs. If in the graph we are currently trying to optimize there is an arm with fewer than *cpa* crossings, then either that arm needs to be changed, or it is a signal that the bound in (12) cannot be achieved.

3 The hatpin

We define a *hatpin* H to be a planar graph consisting of a distinguished point, its head, with a ray emanating from it (e.g., head at $(0,0)$, ray = $\{x = 0, y \leq 0\}$). A graph $G_H(n)$ formed by drawing n hatpins has $V_B = n$ base nodes, $d_B = 1$, and $E_\infty = n$, so (6) gives $R = V_C + 1$, which we maximize by making all the hatpins cross each other, giving $a_H(n) = \binom{n}{2} + 1$. The left-hand figure in Figure 6 below shows a $G_H(4)$. In some drawings we have indicated the heads of the hatpins by small red circles.

Since the optimal hatpin graph $G_H(n)$ is also used in other constructions, we note that it has parameters $V_B = n, d_B = 1, V_C = \binom{n}{2}, V = \binom{n+1}{2}, E_\infty = R_\infty = n, E_f = n(n-1), E = n^2, R_f = \binom{n-1}{2}$, and $R = a_K(n-1) = (n^2 - n + 2)/2$.

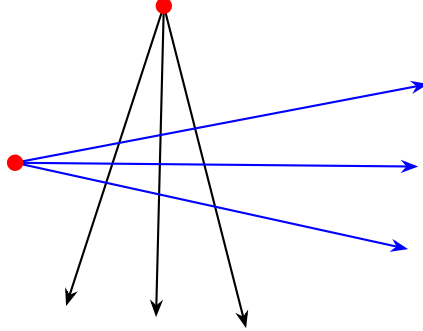


Figure 5: A graph $G_{3V}(2)$ with 14 regions, formed from two 3-armed V's (or Wu's).

$k \backslash n$	0	1	2	3	4	5	6	7	8	...
0	1	1	1	1	1	1	1	1	1	...
1	1	1	2	4	7	11	16	22	29	...
2	1	2	7	16	29	46	67	92	121	...
3	1	3	14	34	63	101	148	204	269	...
4	1	4	23	58	109	176	259	358	473	...
5	1	5	34	88	167	271	400	554	733	...
6	1	6	47	124	237	386	571	792	1049	...
7	1	7	62	166	319	521	772	1072	1421	...

Table 1: Table of $a_{kV}(n)$, the maximum number of regions formed in the plane by drawing n long-legged k -armed V's. The entries are given by (14). Rows 1-4 are [A000124](#), [A130883](#), [A140064](#), [A383464](#), column 2 is [A008865](#), and the OEIS entry for the array itself is [A386481](#).

4 The k -armed V

Our next shape is a long-legged k -armed V, abbreviated kV , which consists of a distinguished point, its tip (e.g., $(0, 0)$), with $d_B = k \geq 1$ rays, or arms, emanating from it, with arbitrary angles between the arms, or any of its images under \mathcal{G}_{aff} . A graph $G_{kV}(n)$ formed by drawing $n \geq 0$ kV 's has $V_B = n$ base nodes and nk arms, with $E_\infty = R_\infty = nk$. For maximizing the number of regions, it turns out to be best to take the arms to be distinct, and forming a fan with a small angular spread, as in Figs. 5 and 6.

From Equations (5) and (6) we obtain

$$E_f = 2V_C, \quad R = V_C + n(k-1) + 1. \quad (13)$$

The crossing number $\kappa(kV)$ is clearly k^2 . We maximize V_C by making every pair of kV 's cross each other in k^2 points, for a total value of $V_C = \binom{n}{2}k^2$, leading to the maximum of

$$R = a_{kV}(n) = \binom{n}{2}k^2 + n(k-1) + 1 \quad (k \geq 1, n \geq 0) \quad (14)$$

regions.² This is easily achieved by taking a $G_H(n)$ hatpin graph and replacing each hatpin by a long narrow copy of a kV (see Fig. 6, which illustrates the construction for four 3-armed V 's). Table 1 shows the values of $a_{kV}(n)$ for $0 \leq k \leq 7$ and $0 \leq n \leq 8$.

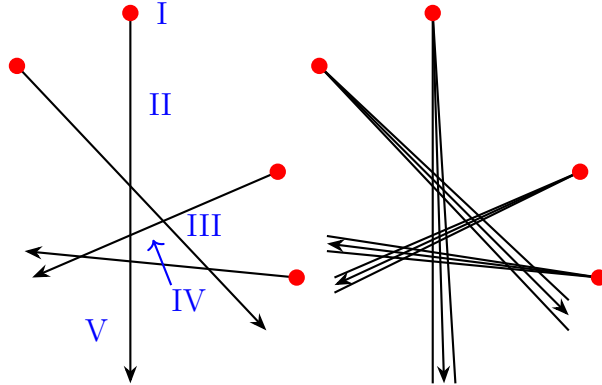


Figure 6: Transforming a hatpin graph $G_H(4)$ to an optimal $G_{3V}(4)$ graph with $a_{3V}(4) = 63$ regions, by replacing hatpins with long narrow 3-armed V 's (or Wu's). The new graph has $V_C = 54$ crossings and $\alpha(3V) = 12$ arms, and a *cpa* of 9, in agreement with (12). (Some of the arrowheads on the right have been omitted for clarity.)

We may verify (14) directly by considering what happens to the different parts of the hatpin graph when the hatpins are replaced by kV s. There are five parts in the hatpin graph, which we denote by I (base nodes), II (finite edges), III (crossing nodes), IV (cells), and V (infinite edges), as shown in Fig. 6. Each crossing node, for example, becomes a $k \times k$ square grid with $\kappa(kV) = k^2$ vertices, $2k(k-1)$ edges, and $(k-1)^2$ regions, and there are $\binom{n}{2}$ such crossing points, as we know from the last paragraph of §3. By combining these counts for the five parts we can verify (14).

5 The k -chain

We define a k -chain (abbreviated kC) to be any continuous plane curve made up of $k \geq 1$ piecewise linear segments, or any image of such a curve under \mathcal{G}_{aff} . A line is a 1-chain, and a V is a 2-chain. Since it can only help in increasing the number of regions, we will assume that the outer line segments (the first and the k th) are infinite. The other segments are required to be finite.

²The $k = 3$ case of (14), $(9n^2 - 5n + 2)/2$ (A140064), was first discovered by Edward Xiong, Jonathan Pei, and David O. H. Cutler on June 24 2025 (see Acknowledgments).

$k \backslash n$	0	1	2	3	4	5	6	7	8	...
0	1	1	1	1	1	1	1	1	1	...
1	1	2	4	7	11	16	22	29	37	...
2	1	2	7	16	29	46	67	92	121	...
3	1	3	14	34	63	101	148	204	269	...
4	1	5	25	61	113	181	265	365	481	...
5	1	8	40	97	179	286	418	575	757	...
6	1	12	59	142	261	416	607	834	1097	...
7	1	17	82	196	359	571	832	1142	1501	...

Table 2: Table of $a_{k\mathcal{C}}(n)$, the maximum number of regions formed in the plane by drawing n k -chains. The entries are given by (16). Rows 1-5 are [A000124](#), [A130883](#), [A140064](#), [A080856](#), [A383465](#), columns 1 and 2 are [A152948](#) and [A386479](#), and the array itself is [A386478](#).

A single k -chain may intersect itself if $k \geq 3$, producing a maximum of $\binom{k-1}{2}$ internal regions and $\sigma(k\mathcal{C}) = \binom{k-1}{2}$ self-intersections.

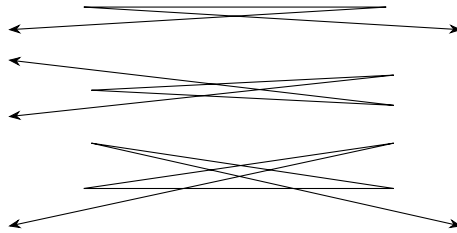


Figure 7: Long narrow drawings of a 3-chain, a 4-chain, and a 5-chain, used in the proof of (16). The first two are essentially unique, but there are two ways to draw the 5-chain—see Fig. 10.

A graph $G_{k\mathcal{C}}(n)$ formed by drawing n k -chains has $V_{\mathcal{B}} = n(k-1)$ base nodes and nk arms, with $d_{\mathcal{B}} = 2$, and $E_{\infty} = 2n$. The basic equation (6) then gives

$$R = V_{\mathcal{C}} + n + 1, \quad (15)$$

just as for the pancake graph (see (8)). So again we must maximize $V_{\mathcal{C}}$, which we can do by first maximizing the self-intersections in each $k\mathcal{C}$, giving $n\binom{k-1}{2}$ intersections, and then using a construction similar to that of the previous section. That is, we draw the individual k -chains as long narrow graphs (as in Fig. 7), and then substitute them into a pancake graph if k is odd (and the k -chain has infinite edges pointing in opposite directions), or into a hatpin graph if k is even (and both infinite edges of the k -chain point in the same direction). See Fig. 8, which illustrates the construction for three 3-chains. As a result we obtain $V_{\mathcal{C}} = n\binom{k-1}{2} + \binom{n}{2}k^2$, and a maximum of

$$R = a_{k\mathcal{C}}(n) = \frac{k^2 n^2}{2} - \frac{3kn}{2} + 2n + 1, \quad (16)$$

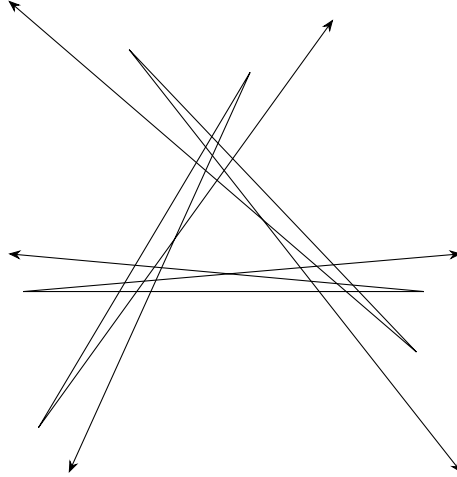


Figure 8: Transforming a pancake graph $G_K(3)$ to an optimal $G_{3C}(3)$ graph with $a_{3C}(3) = 34$ regions, by replacing hatpins by long narrow 3-chains.

regions. The *cpa* for an optimal graph is $2V_C/nk$, which is an integer if and only if $k \leq 2$. Table 2 shows the values of $a_{kC}(n)$ for $0 \leq k \leq 7$ and $0 \leq n \leq 8$.

The $k = 2$ rows of Tables 1 and 2 are of course identical, since a 2-chain is the same as a 2-armed V. The $k = 1$ rows agree except that they are offset from each other by one position. The reason for this is that a 1-chain is a line, whereas a 1-armed V is a hatpin (V's have a distinguished point, lines do not.) But the real surprise is that the $k = 3$ rows of the two tables agree. This will be explained in the next section.

Before leaving this section we mention an as-yet unexplained mystery: Table 2 is very nearly symmetrical: e.g., $a_{4C}(3) = 61$, while $a_{3C}(4) = 63$. This is easily explained by the formula: from (16), $|a_{kC}(n) - a_{nC}(k)| = 2|k - n|$. which is exactly the difference between the numbers of infinite regions in the two optimal graphs. But what is the geometric explanation? Why is the maximum number of regions that can be drawn using n k -chains essentially the same as the number that can be drawn using k n -chains (except for the inevitable difference between the numbers of infinite regions)?

One possible explanation might have been that there is a 1-to-1-correspondence between optimal $G_{kC}(n)$ graphs and optimal $G_{nC}(k)$ graphs. But this is false even in the simplest case. An optimal $G_{1C}(n)$ graph shows n lines in general position in the plane, and the number of such graphs is known for $0 \leq n \leq 9$ (A090338):

$$1, 1, 1, 1, 1, 6, 43, 922, 38609, 3111341, \dots$$

Figure 9 shows the six ways to draw five lines in general position. On the other hand, $G_{kC}(1)$ is a single optimal k -chain (meaning it has $\sigma(n) = \binom{n-1}{2}$ self-intersections) and the number of such graphs for $0 \leq k \leq 5$ is $1, 1, 1, 1, 1, 2, \dots$, the two optimal five-chains being shown in Fig. 10.

So we still do not know if there is a geometrical explanation for the near-symmetry of Table 2.

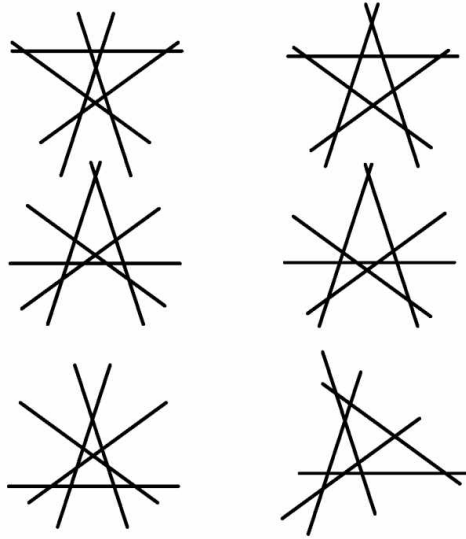


Figure 9: The six ways to draw five lines in general position in the plane [Jonathan Wild and Lawrence Reeves, from [A090338](#)]. (The arrowheads are not shown.) Only the first two correspond to 5-chains (see Fig. 10).

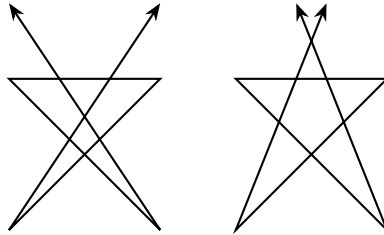
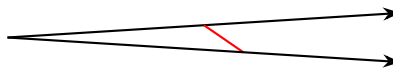


Figure 10: The two optimal 5-chains.

It would also be interesting (see §12) to know further terms in the enumeration of optimal k -chains, and, more generally, the numbers of graphs that achieve any of the values shown in Tables 1 and 2.

6 The long-legged A

Our next shape is a long-legged A, which is a long-legged 2-armed V (§4) with a crossbar joining the two arms, or any of its images under \mathcal{G}_{aff} :



The crossbar need not meet the arms at the same distance from the tip, and the angle between the arms of the V is arbitrary.

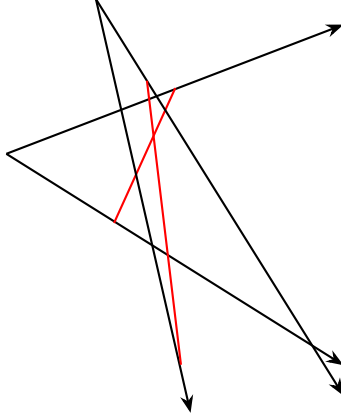


Figure 11: 14 regions can be obtained with two long-legged A 's. The crossbars are shown in red.

Our drawings suggested that the initial values of $a_A(n)$, the maximum numbers of regions achievable with n A 's, for $n = 1, 2$, and 3 , were $3, 14$ (Fig. 11), and 34 , matching the counts for 3-armed V 's and later, the counts for 3-chains. This was not a coincidence!

Theorem 1. *The maximum number of regions that can be formed in the plane by drawing n long-legged 3-armed V 's, or n 3-chains, or n long-legged A 's, is $(9n^2 - 5n + 2)/2$ ([A140064](#)).*

The theorem also applies to long-legged versions of the letters E , Ψ , and \mathbb{W} .

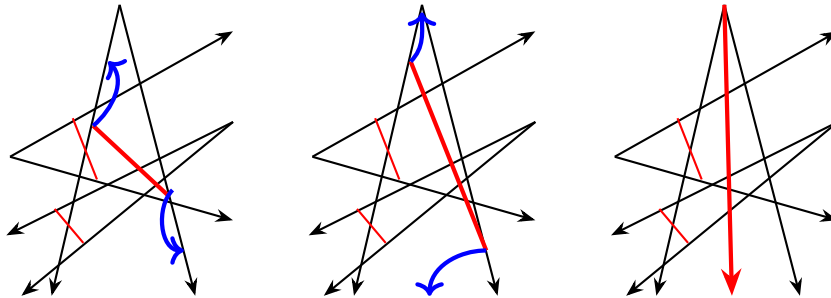


Figure 12: Converting an optimal graph with n long-legged A 's (left) into a graph with n 3-armed V 's (right). The steps do not decrease the number of regions. Reversing the last step (going from right to center) performs the inverse operation.

Sketch of proof. We have already established the theorem for 3-armed V 's (in §4), and for 3-chains (in §5). It remains to consider long-legged A 's.

Let G be an optimal arrangement of n long-legged A 's. Take the crossbar of any A , and suppose the left end of the crossbar is closer to its tip, and the right end is further from its tip (see Fig. 12). Sliding the left end of this crossbar so it is closer to the tip than any crossing node on that arm will not decrease the number of regions.

Similarly, moving the right end of the crossbar so that it is further from the tip than any other crossing node on that arm will also not decrease the number of regions. Finally, we

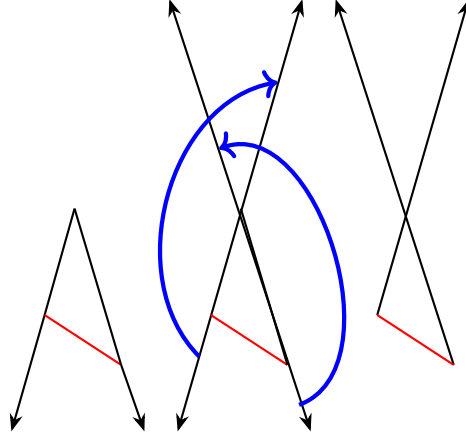


Figure 13: Converting a long-legged A (left) into a 3-chain (right),

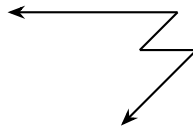
can move the left end of the crossbar so it actually coincides with the tip and the right end so it is cut free from the arm. The A has now become a 3-armed V , and since G was optimal, the number of regions has remained unchanged throughout the process. By repeating this operation for all the A 's in G we turn the A graph into a 3-armed V graph. The converse operation is equally simple.

On the other hand, to convert the long-legged A graph G into an arrangement of 3-chains, we simply apply the transformation shown in Fig. 13. This preserves the number of regions (we invite the reader to apply it to Fig. 11 and check that the result still has 14 regions).

7 The long-legged Z , W , and M

At the other end of the alphabet, for the long-legged Z mentioned in the Introduction (the zig-zag curve of [4]), the basic equation (6) gives (8) again. To maximize V_C we substitute n long narrow copies of Z into the pancake graph, which results in a maximum of $R = a_Z(n) = (9n^2 - 7n + 2)/2$ regions (see A117625). This is exactly the construction used in [4] (although they do not use our counting argument to prove it is optimal).

A natural sequel is worth mentioning. After drawing the first three arms of the Z (as in §1), we may truncate the third arm and add a fourth (infinite) arm that is parallel to the second arm, obtaining this long-legged W (or M) shape:



Our standard analysis (this time substituting into a hatpin graph) shows that the maximum number of regions is $a_W(n) = 8n^2 - 7n + 1$ (A125201). Figure 14 illustrates $a_W(2) = 19$.

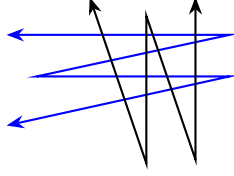


Figure 14: Two long-legged W's divide the plane into 19 regions.

8 The constrained long-legged \bar{L} and \bar{X}

In this section we discuss our first two shapes from the similarity family, \bar{L} and \bar{X} , both of which we are able to solve.

8.1 The constrained long-legged \bar{L}

With no restriction on the angle, a long-legged L would be indistinguishable from a long-legged V . We define a *constrained long-legged \bar{L}* to consist of a distinguished point, its center (e.g., $(0,0)$), from which two perpendicular rays emanate (e.g., $\{y = 0, x \geq 0\}$ and $\{x = 0, y \geq 0\}$), or any of the images of such a figure under the similarity group \mathcal{G}_{sim} .

Two \bar{L} 's can intersect in at most $\kappa(\bar{L}) = 3$ points, so $V_C \leq 3\binom{n}{2}$ and then (6) gives

$$R \leq 3\binom{n}{2} + n + 1 = (3n^2 - n + 2)/2 \quad (\text{A143689}) . \quad (17)$$

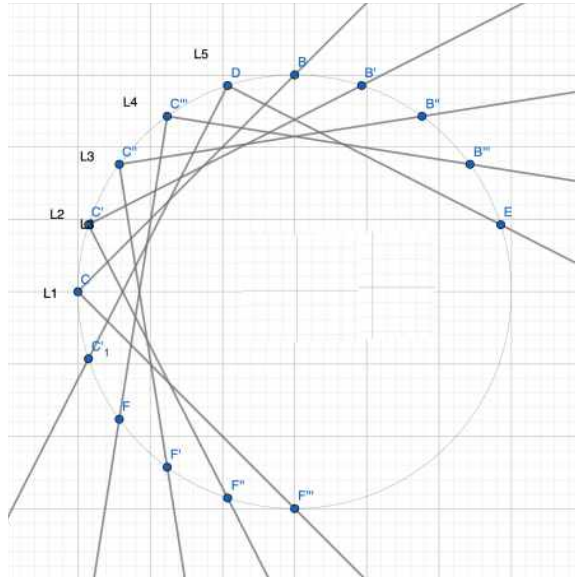


Figure 15: The construction of n constrained long-legged \bar{L} 's, showing the case $n = 5$. There are 36 regions. (The arrowheads have been omitted.)

Equality in (17) can be achieved by modifying the standard construction for drawing n squares with the maximum number of regions (see [A069894](#)). This construction starts

by marking $4n$ equally-spaced points P_0, \dots, P_{4n-1} around the circumference of a circle. To get an optimal arrangement of n squares, we would take the squares with vertices $\{P_i, P_{i+n}, P_{i+2n}, P_{i+3n}\}$ for $i = 0, 1, \dots, n-1$. To get an optimal arrangement of n \bar{L} 's, we take the \bar{L} 's formed by the top left corners of these squares. That is, we draw an \bar{L} centered at P_i with arms $P_i - P_{i+n}$ and $P_i - P_{i+3n}$, for $i = 0, \dots, n-1$. Figure 15 shows the construction when $n = 5$. In general the graph contains $2n$ infinite regions, there are n rows of $n-1$ cells each, and a further triangle of $(n-1)(n-2)/2$ cells, for a total of $R = a_{\bar{L}}(n) = (3n^2 - n + 2)/2$ regions. For $n \geq 0$ the values are 1, 2, 6, 13, 36, 52, 71, ... (A143689). The OEIS entry makes no mention of this geometric application, so this result may be new.

There are $V = n + 3\binom{n}{2} = n(3n-1)/2 = R - 1$ vertices, which is a pentagonal number (A000326—). The presence of pentagonal numbers can be explained as follows. The familiar picture of the pentagonal numbers ([4, p. 380], for example) shows a pentagonal array of dots divided into successive shells of 1, 4, 7, 10, 13, ... dots. Careful examination of the grid of points formed by the above construction (as in Fig. 15) reveals exactly the same shells of points.

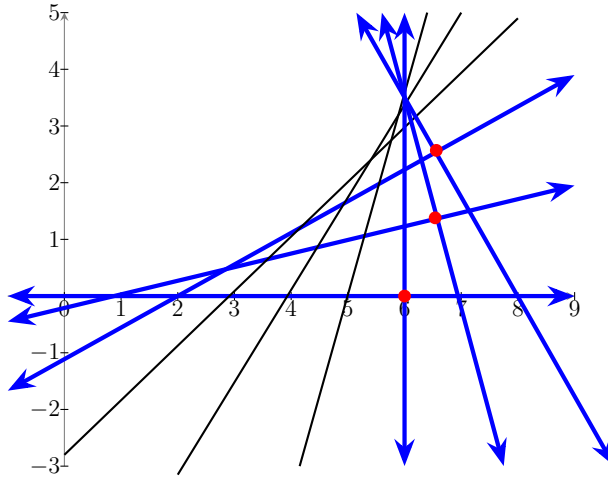


Figure 16: Dividing the plane into the maximum number of pieces using n \bar{X} 's (or coordinate frames). For $n = 3$, draw a grid of lines λ_t defined by (9) with $\theta = \pi/(4n) = \pi/12$ and $t = 0, \dots, 3n-1 = 8$. The three \bar{X} 's (centered at the red dots, and with blue axes) are $\lambda_0 \cup \lambda_6$, $\lambda_1 \cup \lambda_7$, and $\lambda_2 \cup \lambda_8$. An enlargement of the figure will show that, although it is not clear from this illustration, there is no point where any three of the lines intersect.

8.2 The constrained long-legged \bar{X}

A *constrained long-legged \bar{X}* consists of a distinguished point, its center, e.g., $(0, 0)$, from which two perpendicular lines (its arms, or axes) emanate (e.g., $x = 0$ and $y = 0$), or any of the images of this figure under the similarity group \mathcal{G}_{sim} .

A graph $G_{\bar{X}}(n)$ with n \bar{X} 's is also a pancake graph $G_{\kappa}(2n)$ with $2n$ lines, so (1) gives

$$a_{\bar{X}}(n) \leq a_{\kappa}(2n) = 2n^2 + n + 1 \quad (\text{A084849}) . \quad (18)$$

Two \bar{X} 's can intersect in at most $\kappa(\bar{X}) = 4$ points, so $V_C \leq 4\binom{n}{2}$, and then (6) also gives $R \leq 2n^2 + n + 1$.

We can indeed achieve equality in (18) by modifying the construction of pancake graphs given in §2. To construct a $G_{\bar{X}}(n)$ containing n copies of \bar{X} , set $\theta = \pi/(4n)$, and let λ_t denote the line (9). Draw the lines λ_t for $t = 0, 1, \dots, 3n - 1$ (now we need more of these lines than when we constructed the pancake graph). The t th copy of \bar{X} is formed from the lines λ_t and λ_{t+2n} for $t = 0, \dots, n - 1$. Figure 16 illustrates the construction for $n = 3$. Of all our constructions, this one seems to be the most likely to have applications, possibly to some abstract version of the Gerrymandering problem.

9 The constrained long-legged \bar{T} and \bar{A}

Up to this point in our investigations we were able to analyze the shapes by hand, using pencil and paper and traditional drawing instruments. But the next two shapes in the similarity family, \bar{T} and \bar{A} , appear to be more difficult and we invoked the aid of the computer (and even so, we will only end up with guesses at the solutions).

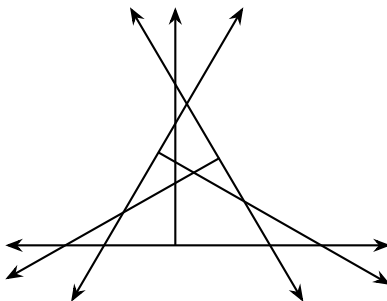


Figure 17: Three constrained long-legged \bar{T} 's can divide the plane into 19 regions. It is impossible to add a fourth \bar{T} that meets each of the first three in 4 points.

9.1 The constrained long-legged \bar{T}

A *constrained long-legged \bar{T}* consists of a distinguished point, its center (e.g., $(0, 0)$), which is at the intersection of a line and a perpendicular ray (e.g., $y = 0$ and $\{x = 0, y \leq 0\}$), or any of the images of this figure under the similarity group \mathcal{G}_{sim} .

Two such \bar{T} 's can intersect in at most four points, our standard analysis gives $R \leq V_C + 2n + 1 \leq 4\binom{n}{2} + 2n + 1$, and so

$$a_{\bar{T}}(n) \leq 2n^2 + 1 . \quad (19)$$

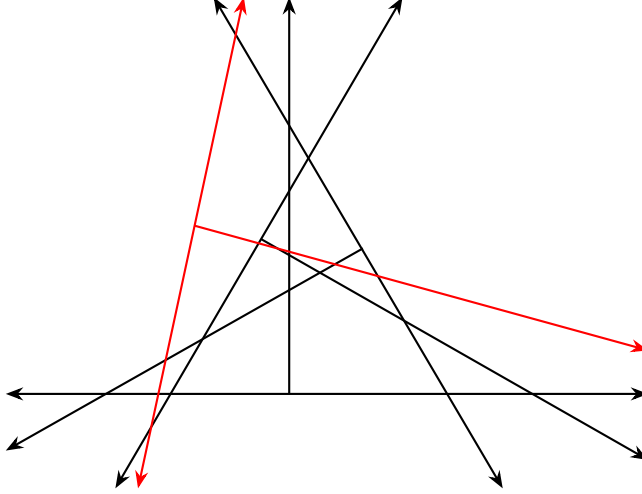


Figure 18: Four constrained long-legged \bar{T} 's can divide the plane into 32 regions. The first three are the same as in Fig. 17, and the fourth (which meets one of the first three in only three points, not four) is drawn in red.

Figure 17 illustrates $a_{\bar{T}}(3) = 19$. However, the configuration of three \bar{T} 's shown in Fig. 17 is essentially unique, and one can check (by hand) that there is no way to add a fourth \bar{T} that meets each of the first three in four points. So equality does not hold in (19) for $n \geq 4$. For $n = 4$ the best we can achieve is 32 regions (Fig. 18).

At this point we used a computer to search for optimal configurations with n copies of \bar{T} . Our Python program used simulated annealing: starting from a randomized initial configuration, we repeatedly perturbed the centers and angles of the \bar{T} 's with noise, seeking to increase the number of crossings and hence the number of regions.

The results suggest there is a simple formula for the optimal solution $a_{\bar{T}}(n)$, which is best seen by tabulating the difference $2n^2 + 1 - a_{\bar{T}}(n)$. This difference, for $0 \leq n \leq 12$, appears to be

$$0; 0, 0, 0; 1, 2, 3; 5, 7, 9; 12, 15, 18; 22, 26, 30; \quad (20)$$

(writing a semicolon after terms where n is a multiple of 3), which is equal to $(\lambda - 1)n - 3\binom{\lambda}{2}$ where $\lambda = \lceil \frac{n}{3} \rceil$. If correct, this would imply that $a_{\bar{T}}(n)$ is equal to

$$2n^2 + n + 1 - \lambda n + 3\binom{\lambda}{2} \quad (\text{A389614}). \quad (21)$$

To prove that this formula is correct, ideally we would like an explicit construction that achieves it for all $n \geq 0$, and a proof that no greater value is possible. At present we have neither of these things for $n > 4$, so we leave (21) as a conjecture.

9.2 The constrained long-legged \bar{A}

The *unconstrained* long-legged A was discussed in §6, where we showed that it is equivalent to a three-armed V . A *constrained long-legged \bar{A}* is defined to be a long-legged A in which the ends of the crossbar are equidistant from the tip, or any image of such a figure under \mathcal{G}_{sim} .

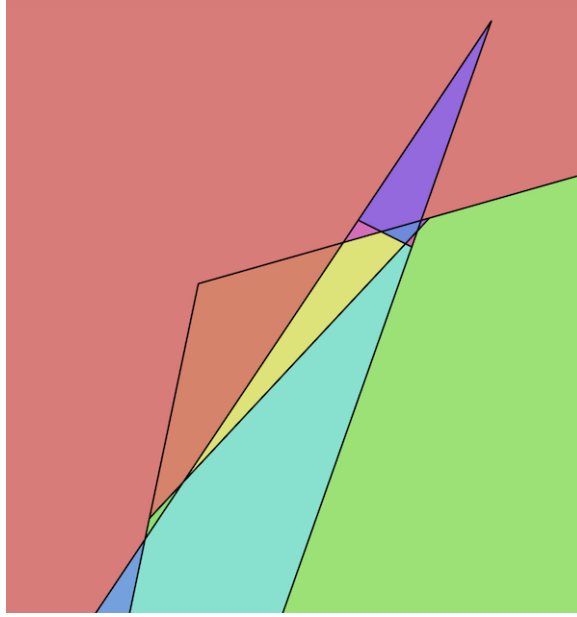


Figure 19: Two constrained \bar{A} 's can intersect in 8 points, and divide the plane into $a_{\bar{A}}(2) = 13$ regions. (In this picture one \bar{A} has a purple tip, the other a brown tip. The arrowheads are not shown.)

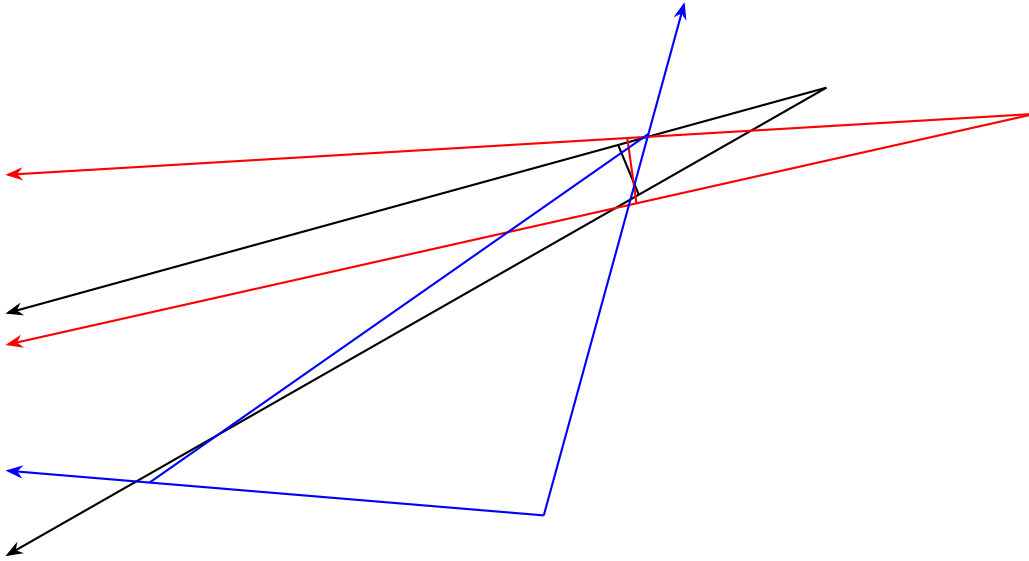


Figure 20: Three constrained \bar{A} 's can divide the plane into 30 regions.

For both the unconstrained A and the constrained \bar{A} , the degrees of the base nodes are not all equal. For both shapes, there are three base nodes: the tip, which has degree 2, and the two crossbar nodes, which have degree 3.

Two constrained \bar{A} 's can intersect in a maximum of $\kappa(\bar{A}) = 8$ points, and divide the plane into $a_{\bar{A}}(2) = 13$ regions. This construction was not easy to find (it was discovered by our program), so we provide a colored illustration in Fig. 19. This shape \bar{A} was by far the most

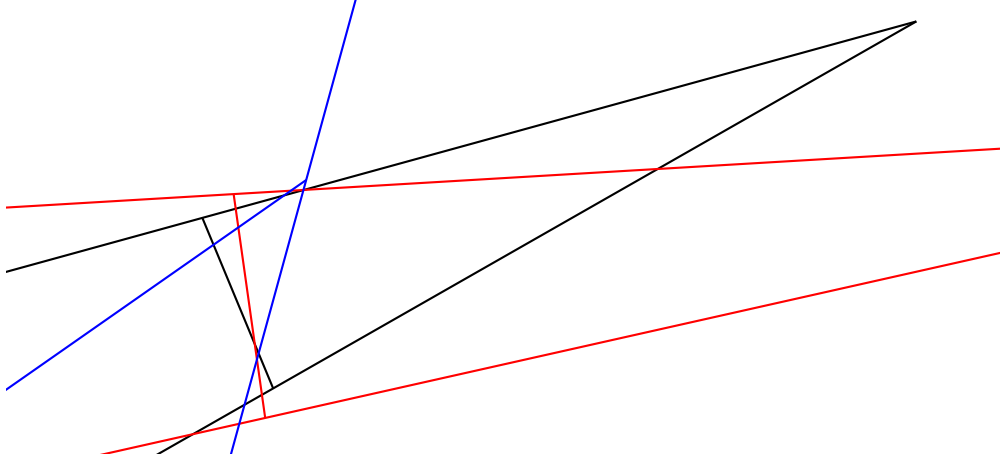


Figure 21: Enlargement of the portion of Fig. 20 where the three crossbars come together.

difficult that we studied.

From (6) we obtain

$$a_{\bar{A}}(n) \leq 4n^2 - 2n + 1 \quad (\text{A054554}) . \quad (22)$$

However, it appears that equality does not hold in (22) for $n > 2$. We modified the program used in the previous section to apply to this problem. For $0 \leq n \leq 5$ the maximum number of regions we found were

$$1, 3, 13, 30, 53, 83 . \quad (23)$$

In particular, for three \bar{A} 's, it appears that only 23 crossings are possible, not 24, giving 30 regions rather than 31. The numbers in (23) match [A330451](#) for $n > 0$, which would suggest that perhaps $a_{\bar{A}}(n)$ is equal to $\lfloor \frac{10n^2}{3} \rfloor$ for $n > 0$. Nonetheless, we are not at all sure that even this formula is correct. The difficulty is that the putatively optimal graphs contain extremely small regions, approaching the precision limit of the computer. Even for $n = 3$ the graph (shown in Fig. 20 and enlarged in Fig. 21) contains regions that are barely visible to the naked eye.

For larger n we will simply give decimal approximations to the coordinates of the \bar{A} 's, as found by our program (see Table 3). In the table, n is the number of \bar{A} 's, R is the number of regions, V_C is the number of crossings, and each \bar{A} is represented by a row of five numbers: the coordinates (x, y) of the tip, the angles ϕ_1 and ϕ_2 of the two arms emanating from the tip, measured in radians counter-clockwise from the positive x axis, and the distance d from the tip to either end of the crossbar.

10 Finite shapes

10.1 Convex polygons

The k -sided convex polygon, $k \geq 3$, abbreviated kP , is the last of our shapes in the affine family. kP is a convex k -gon (e.g., a regular k -gon) or any of its images under \mathcal{G}_{aff} . Since

$n (R, V_C)$	x	y	ϕ_1	ϕ_2	d
1 (3, 0)	0.	0.	4.450589	4.974188	1
2 (13, 8)	-.263978	-5.678431	2.158733	1.90873	4.2
	-5.389931	-1.072469	6.006142	8.060452	4.2
3 (30, 23)	15.516576	4.381652	3.410106	3.660106	4.081685
	19.452315	3.885769	9.483921	3.362481	7.712253
	10.175527	-3.701396	3.058488	1.303012	7.475461
4 (53, 44)	-8.802700	0.363764	2.607352	1.213715	6.281140
	-6.521180	6.363038	3.491610	3.791215	7.556620
	-20.226745	4.948778	.0311271	6.011715	6.825288
	-17.449754	-2.062545	1.044651	.794651	6.535819
5 (83, 72)	-3.192510	9.752208	4.057894	2.632951	4.489527
	-3.416682	9.957015	2.799844	4.145734	4.560146
	-2.792041	4.279350	2.560860	2.208129	3.793355
	-8.071091	-0.035548	1.459585	1.209585	6.835
	-3.703641	3.970027	2.331950	2.081950	3.33617

Table 3: Coordinates of best arrangements of $n \bar{A}$'s presently known. See text for explanation of symbols.

$V_B = k$ and $v_B = 2$, (10) tells us that $R = V_C + 2$. Two such polygons can intersect in at most $2k$ points, so $V_C \leq 2k \binom{n}{2}$. This is easily achieved, so

$$a_{kP}(n) = kn^2 - kn + 2 \quad (n \geq 1), \quad \text{with } a_{kP}(0) = 1. \quad (24)$$

The solutions for $k = 3, 4$, and 5 (for the triangle, square or convex quadrilateral, and pentagon) are given in sequences [A077588](#), [A069894](#), and [A386485](#). It was a slight surprise to discover that taking $k = 1$ and $k = 2$ in (24) matched [A386480](#) and [A051890](#), which are the numbers of regions attainable with n circles (see §10.3) and n ellipses, respectively. Most surprising, however, was the case $k = 8$, which we discuss in the next subsection.

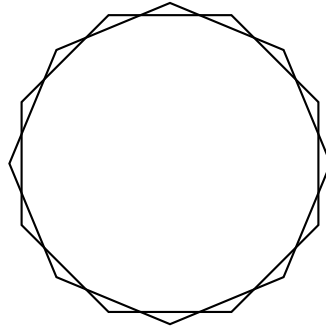


Figure 22: Two regular octagons divide the plane into 18 regions.

10.2 The octagon and concave quadrilateral

For a convex octagon, the values of $a_{8P}(n)$ are 1, 2, 18, 50, 98, 162, 242, ... that is, $2(2n - 1)^2$ for $n > 0$. Figure 22 illustrates $a_{8P}(2) = 18$. Remarkably, this sequence also matches [A077591](#), whose definition is the maximum number of regions obtainable in the plane by drawing n concave quadrilaterals. The latter is illustrated in Figure 23 for $n = 2$ (and which also has 18 regions). Since there is no obvious connection between the two dissections, the result *may* be just a coincidence.

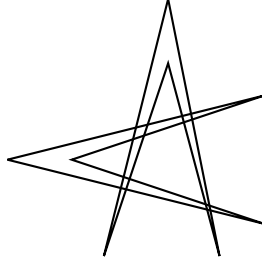


Figure 23: Two concave quadrilaterals also divide the plane into 18 regions. Is it just a coincidence that the maximum number of pieces that can be obtained with n (convex) octagonal cuts is the same as can be obtained with n concave quadrilateral cuts? We do not know!

10.3 The circle

Although our basic equation (10) would not apply to curved shapes with arbitrarily many twists, it does apply to the circle and figure-8. These and the other shapes discussed below all belong to the similarity family.

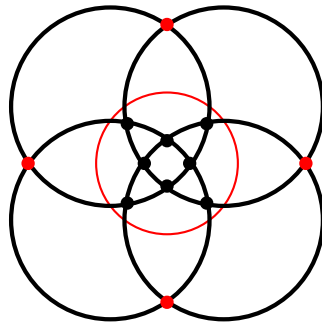


Figure 24: Four circles (black) can divide the plane into 14 regions. There are four base nodes (red) and eight crossing nodes (black). The centers (not shown) of the black circles are four equally spaced points around the thin (red) circle, which is the starting point of the construction, but is not part of the final graph.

For $n \geq 2$ circles the maximum number of regions, $a_{\text{O}}(n) = n^2 - n + 2$, is well known ([A014206](#), [A386480](#)), but we have not seen an explicit construction mentioned, so we give one here, and then show how our basic formula when applied to it gives the correct answer. We start by placing the n centers at n equally-spaced points around an initial circle of radius ρ , say, and then draw circles of radius $8\rho/5$ around these centers. The initial circle, its center point, and the n points that we marked on it are not part of the graph. This choice of radius ensures that each circle cuts every other circle in two points. Figure 24 illustrates the case $n = 4$.

The boundary of the resulting graph contains n points where the circles intersect. We take these to be the base nodes. There are a further $V_c = n(n-2)$ crossing nodes, for a total of $V = n(n-1)$ vertices, and $E_f = 2n(n-1)$ edges, and (10) confirms that $R = n^2 - n + 2$.

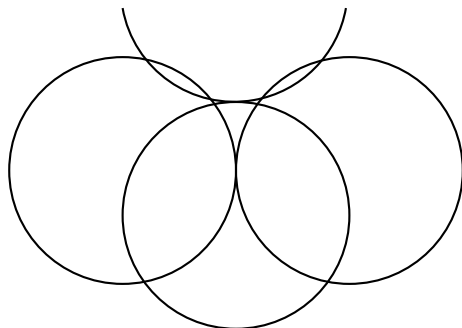


Figure 25: Two figure 8's can divide the plane into 12 regions

10.4 The figure 8

A figure 8 shape consists of two tangential circles of equal but arbitrary radius. A graph with n 8's contains $2n$ circles, and so $a_{\mathcal{O}}(2n)$ from the previous section is an upper bound on $a_8(n)$. However, we cannot achieve all the intersections needed to achieve that bound, since the two constituent circles of each 8 cannot properly intersect. We conjecture that the effect of this constraint is simply to reduce the number of crossings by 2 for each figure 8, and so the solution for the 8 is conjecturally that $a_8(n) = 4n^2 - 3n + 2$ ([A386486](#)). The conjecture appears to be true at least for $n \leq 3$. Figure 25 illustrates $a_8(2) = 12$.

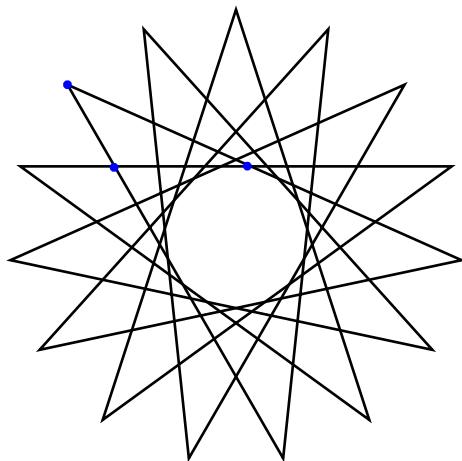


Figure 26: Three pentagrams can divide the plane into 77 regions.

10.5 The pentagram and hexagram

A *regular* pentagram or hexagram is based on 5 or 6 equally spaced points around a circle. To attain the maximum number of regions we will use regular figures, but our analysis applies equally to non-regular figures. A single pentagram (regular or non-regular) has 5 base nodes, the exterior vertices, with degree $d_B = 2$, and 5 self-intersections, in the interior. Two pentagrams can meet in at most 20 points, so with n pentagrams we have $V_C \leq 5n + 20\binom{n}{2}$. For n pentagrams our basic equation (10) then gives $R \leq V_C + 2 \leq 5n + 20\binom{n}{2} + 2 =$

$10n^2 - 5n + 2$ ([A383466](#)), a bound which is easily achieved using regular pentagons based on $5n$ equally spaced points around a circle. The construction is illustrated for $n = 3$ in Fig. 26. To verify the number of regions, note that each of the base nodes is a vertex of a triangular region (indicated by the three blue dots in Fig. 26) containing $2n - 1$ cells. We were led to investigate pentagons because an optimal 5-chain (§5) necessarily contains a pentagon (see Figs. 7 and 10).

A hexagram initially contains two disjoint triangles and is not a connected graph, which would violate the assumption that our shapes are connected, but *is* connected if we take the self-intersections into account. The analysis is similar to that of the pentagon, so we just state the result: the maximum number of regions that can be attained in the plane by drawing n hexagrams is $2(6n^2 - 3n + 1)$ ([A386477](#)).

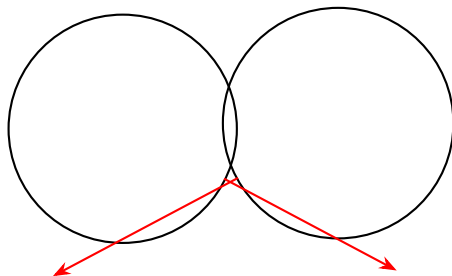


Figure 27: Two lollipops can intersect in at most 7 points and can divide the plane into 10 regions. The sticks of the lollipops are colored red.

11 The lollipop

Although it does not quite meet our conditions, since it is both curved and infinite, we cannot resist ending with a brief analysis of the lollipop shape (\mathcal{Q}). Formally, a lollipop is a circle together with a ray (the *stick*) emanating from its center but with the portion of the ray inside the circle omitted, or any image of such a shape under \mathcal{G}_{sim} . Besides its intrinsic appeal, the lollipop is also a possible candidate for a long-legged version of both the letters P and Q.

Two lollipops can meet in a maximum of $\kappa = 7$ points (Fig. 27). Equation (6) applies to this shape, and implies that the maximum number of regions possible with n lollipops is

$$R \leq \frac{7n^2 - 5n + 2}{2} \quad (\text{A389608}) . \quad (25)$$

This can be achieved for $n \leq 3$ (Fig. 28), though it is already unclear what is happening when $n \geq 4$. As in §9.2, computational methods may be used, but the delicate nature of the optimal solutions makes them highly sensitive to numerical errors.

12 Open problems

1. Find optimal graphs for the four shapes that we left unfinished: the constrained long-legged letters \bar{T} (§9.1) and \bar{A} (§9.2), the figure 8 (§10.4), and the lollipop (§11).

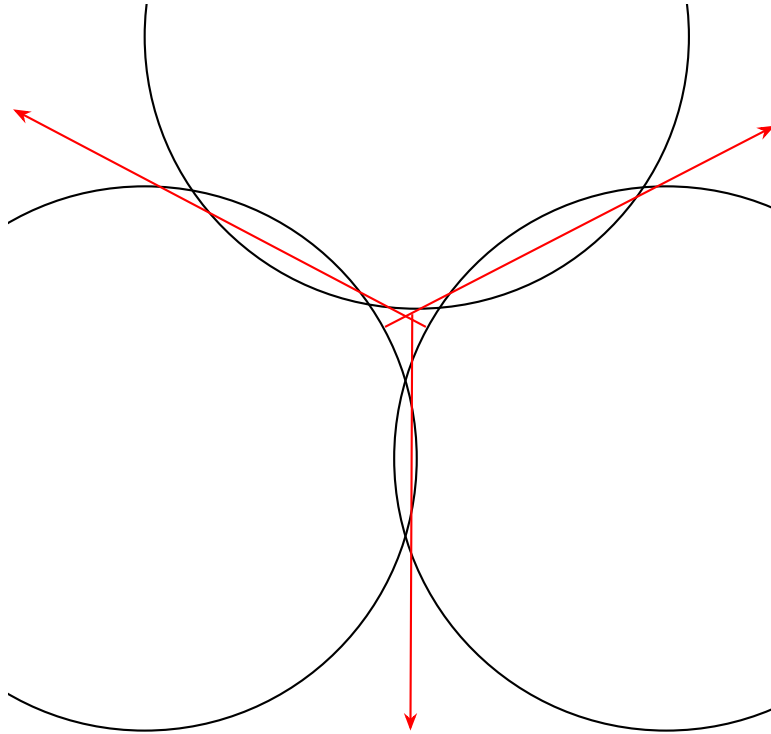


Figure 28: With each pair intersecting in 7 points, three lollipops can divide the plane into 25 regions.

2. *Enumerative Geometry.* We have already mentioned (in §5) the sequence [A090338](#), which gives the number of ways to draw n lines in general position in the Euclidean plane, and which is also the number of ways to cut the plane into the maximum number of pieces with n straight cuts. The values are known for $n \leq 9$. If we omit “in general position”, and just ask for the number of ways to draw n lines in the plane, there are more possibilities, and the values ([A241600](#)) are known only for $n \leq 7$. For $n = 3$, for example, there are four possibilities: three parallel lines, two parallel lines and a line cutting both, three lines through a point, and three lines in general position. There are still more ways if we restrict the question to a disk (a pizza, say). For $0 \leq n \leq 6$ it appears that the values are 1, 1, 2, 5, 19, 130, 1814 ([A272906](#)), although the last term is unconfirmed. There has been no progress on either of the last two questions for ten years.
3. More generally, for any shape S for which we have determined the maximum number of regions $a_S(n)$ (which includes all the entries in Tables 1 and 2), we may ask for the number of distinct graphs having that many regions. The case when S is a circle has been studied by J. Wild in [A250001](#) and [A288554](#). He shows that the numbers of distinct planar graphs composed of n overlapping circles that divide the plane into $n^2 - n + 2$ regions are respectively 1, 1, 4, 45, 5102 for $n = 1, \dots, 5$. The four possibilities for $n = 3$ are shown in Fig. 29. One of the 45 is shown in Fig. 24).

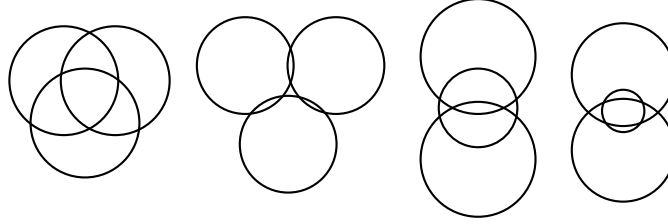


Figure 29: Three circles can divide the plane into a maximum of 8 regions, and this can be done in 4 ways. (Only the first is a Venn diagram.)

4. Is there a geometric explanation for the near-symmetry of Table 2 (§5)?
5. Is there a geometric explanation for the apparent coincidence mentioned in §10.2?
6. *Geometrical Configurations*. In the classical theory of Geometrical Configurations [6], [7, Chap. III, *Projective Configurations*], [9], a configuration with symbol (p_λ, ℓ_π) is an arrangement of p points and ℓ lines in the plane such that each point is incident with λ lines, and each line is incident with π points.

Our graphs $G_S(n)$ satisfy this condition provided the number of crossings per arm (cpa) is constant, as it is in most cases considered here, and if so then $G_S(n)$ is a geometrical configuration with $p = V_C$, $\lambda = 2$, $\ell = \text{number of arms } \alpha(S)$, and $\pi = cpa$.

For example, the optimal constrained long-legged \bar{T} graphs discussed in §9.1, which we showed do not exist for $n > 3$, would have formed configurations with $p = 4\binom{n}{2}$, $\lambda = 2$, $\ell = 2n$, and $\pi = 2(n - 1)$ for integers $n \geq 1$. Could the classical theory have resolved that question? Does the theory have any other application to our problems? Grünbaum's book [6], although it is mostly concerned with configurations of type (p_λ, p_λ) , contains a large number of striking illustrations similar to those in the present article.

13 Acknowledgments

N.J.A.S. mentioned the subject of this paper in a Research Experience for Undergraduates seminar at Rutgers University on June 24 2025. Following the talk, three participants in the seminar, Edward Xiong, Jonathan Pei, and David O. H. Cutler, solved the 3-armed V problem (see §4). Their solution led us to the edge-vertex formula of (5), which underlies all our calculations. We thank Susanna S. Cuyler, Sean A. Irvine, Gareth McCaughan, Scott R. Shannon, and Jonathan Wild for comments on the manuscript, and Scott R. Shannon for his dramatic illustrations of the pentagram and hexagram graphs (see [A383466](#) and [A386477](#)). Figure 15 was drawn using GeoGebra.

References

- [1] B. Bollobás, *Modern Graph Theory*, Springer, 1998.

- [2] L. Comtet, *Advanced Combinatorics*, Reidel, 1974.
- [3] M. Gardner, *New Mathematical Diversions from Scientific American*, Simon and Schuster, 1966.
- [4] R. L. Graham, D. E. Knuth, and O. Patashnik, *Concrete Mathematics*, Addison-Wesley, 2nd ed., 1994.
- [5] B. Grünbaum, Venn diagrams and independent families of sets, *Math. Mag.*, **48** (1975), 12–23.
- [6] B. Grünbaum, *Configurations of Points and Lines*, Graduate Studies in Math. **103**, Amer. Math. Soc., 2009.
- [7] D. Hilbert and S. Cohn-Vossen, *Geometry and the Imagination*, Chelsea, NY, 1952; 2nd Ed., Springer, 1996.
- [8] I. Lakatos, *Proofs and Refutations: The Logic of Mathematical Discovery*, Cambridge, 1976.
- [9] F. Levi, *Geometrische Konfigurationen*, Hirzel, 1929.
- [10] OEIS Foundation Inc. (2025), *The On-Line Encyclopedia of Integer Sequences*, <https://oeis.org>.
- [11] F. Ruskey and M. Weston, A survey of Venn diagrams, *Electronic J. Combin.*, Dynamic Surveys **5**, 2005.
- [12] A. M. Yaglom and I. M. Yaglom, *Challenging Mathematical Problems with Elementary Solutions. Vol. I. Combinatorial Analysis and Probability Theory*, Dover Publications, 1987.
- [13] W. B. Yeats, *The Collected Poems of W. B. Yeats*, Macmillan, 1956.

Keywords: pancake cutting, plane dissection, bent line, zig-zag, configuration, cookie cutter
2010 Mathematics Subject Classification: Primary 05C10, Secondary 05C63, 52C30